JOURNAL OF COMPUTATIONAL PHYSICS 108, 159–174 (1993)

Basis Function Calculations for the Massive Schwinger Model in the Light-Front Tamm–Dancoff Approximation

YIZHANG MO AND ROBERT J. PERRY

Department of Physics, The Ohio State University, Columbus, Ohio 43210

Received May 19, 1992

We use light-front field theory to study the massive Schwinger model. After making a Tamm–Dancoff truncation of Fock space so that no more than four particles are allowed in any state, the coupled light-front Tamm–Dancoff integral equations for charge zero states are solved by expanding the two-particle and four-particle amplitudes in a finite basis, thereby converting the original equations into a simple matrix equation. By retaining the four-particle sector we are able to study both the lowest energy boson of the theory and the first excited state, which for massless fermions is a scattering state of two ground state bosons. Known results for the massless Schwinger model are accurately reproduced with reasonably small bases, and existing numerical results for the massive model are reproduced and improved. The rich physics of the Schwinger model is used to elucidate several simple problems in the use of basis functions to solve Hamiltonian field theories.

1. INTRODUCTION

Light-front field theory (LFFT) provides a physically intuitive method of analyzing relativistic bound states [1, 2]. When one makes a Tamm–Dancoff [3, 4] truncation of the infinite dimensional Fock space required by local field theory, limiting the number of constituents [5, 6] any state can have, the resultant light-front Tamm–Dancoff (LFTD) approximation [7, 8] may provide a powerful tool for the analysis of hadrons and nuclei. Of course, such a truncation is artificial and one must ensure that the limit in which the entire Fock space is retained can be recovered from calculations in a truncated space [8]. In the case of the super-renormalizable Schwinger model [9–11] and its massive fermion extension [12, 13], this limit can be taken in an extremely naive fashion. One can simply use the canonical Hamiltonian, without ever needing to study its renormalization as momentum and particle number cutoffs change. It has long been appreciated that super-renormalizable Hamiltonians change with momentum cutoffs in a trivial manner [14]. It has simply been observed, first by Bergknoff [15], that the low energy states of the massive Schwinger model are approximated well in LFFT (not in equal-time field theory (ETFT)) even when the cutoff on particle number is extremely severe. For example, throughout the range of fermion mass, the lowest energy boson is almost a pure fermion–antifermion bound state. This makes the Schwinger model unsuitable for the study of many of the most difficult and interesting renormalization problems in LFTD; however, it also makes this model an ideal development ground for numerical techniques that are required before one can attack these renormalization problems.

LFFT has several advantages over conventional ETFT. First and most importantly, in light-front coordinates vacuum degrees of freedom are easily isolated and removed, forcing the vacuum to be trivial. If spontaneous or dynamical symmetry breaking do not occur, the bare vacuum is the physical vacuum. If they do occur, this is certainly not the case; however, one can attempt to reproduce the effects of vacuum condensates with effective interactions [16–20]. This effort is tremendously simplified by the fact that vacuum degrees of freedom are readily separated from the degrees of freedom that compose physical particles built on the vacuum. Second, the light-front Lorentz boost operators do not contain interactions [2], so that the truncation of Fock space according to particle number does not violate boost invariance. In $1+1$ dimensions this means that a Tamm–Dancoff truncation does not violate Lorentz covariance [8]. In addition, LFFT contains fewer fermionic degrees of freedom than ETFT, and in a light-cone gauge it contains only physical gauge degrees of freedom; but the price is a more complicated Hamiltonian.

In this paper, we apply LFTD to the massive Schwinger model. The original massless Schwinger model [9–11] and its massive extension [12, 13] have long been considered as showcases for important aspects of gauge field theory such as confinement and bosonization. As discussed above, in some ways the Schwinger model is artificially simple; therefore, we only attempt to draw a few simple lessons from our study and do not advertise it as a significant test of this approach for solving gauge theories in $3+1$ dimensions.

0021-9991/93 $5.00

Nonetheless, our results, added to those from studies [21] of the Yukawa model in $1+1$ dimensions, where basis functions and momentum space grids were used to solve LFTD equations, are encouraging. Our goal is to accurately reproduce the low-lying states of the Schwinger model for all values of the fermion mass, m_f (i.e., all values of the coupling, e).

Bergknoff [15] first applied LFFT to the Schwinger model. He solved the LFFT Hamiltonian equations numerically in a Fock space truncated to two particles, obtaining excellent results for the ground state boson throughout the entire range of fermion mass. He did not discuss the numerical techniques employed for these calculations. In order to study the first excited state he discovered that for light fermions (i.e., strong coupling) it is necessary to include the four-particle sector of Fock space, and he employed trial wave functions to find the first excited state. Since the lowest energy state is odd under charge conjugation, while the second state is even, one can minimize the energy for states of each symmetry to obtain the ground state boson and the first excited state. Our calculations can be viewed as a simple extension of Bergknoff's calculations to include a larger space of trial wave functions, and we strongly encourage the reader to study Bergknoff's paper before studying our paper in detail. His work was largely restricted to states in the two-particle sector, although his variational wave functions were also adequate for a study of the first excited state very near the massless limit. For extremely massive quarks (i.e., weak coupling) it is also fairly easy to construct reasonable trial wave functions for the first two states, because both are nonrelativistic and both are almost pure two-particle states.

Discretized light-cone quantization (DLCQ) has also been used to study the massive Schwinger model [22–24]. DLCQ [25] is quite successful for most couplings; however, errors grow noticeably as one approaches the strong-coupling limit. The reasons for this are easily understood, because DLCQ solves the LFFT integral equations by using equal-spaced grids in momentum space [26, 21]. As we shall discuss, near the massless limit the analytically determined boundary conditions that wave functions must satisfy near the edges of momentum space [27, 15] are not easily reproduced, and errors near these boundaries have noticeable effects on eigenvalues. This is a problem associated with short distance structure in position space. An equal-time lattice gauge calculation has been completed by Crewther and Hamer [28]. Their results also suffer from increasing inaccuracy in the strong coupling region because of problems that are complementary to those that occur for DLCQ. While the ground state boson is tightly bound, the first excited state consists of two weakly bound bosons whose wave function has a large spatial extension in the strong coupling limit. An accurate representation of the first excited state requires one to resolve structure at both large and small distance scales, and this is typically difficult for grids in either position or momentum space. Finally we should mention the numerical studies of Ma and Hiller [29]. They studied several numerical techniques, but only considered the theory truncated to one fermion–antifermion pair. As we discuss below, when the fermion mass approaches zero the first excited state is almost purely four-particle and the two-particle approximation is valid only for the ground state boson. While it is relatively easy to reproduce the mass and wave function for the ground state boson, there remains plenty of room to improve the calculation of the first excited state in the Schwinger model, especially near the massless limit. This exercise is useful preparation for the more ambitious challenge of solving gauge theories in $3+1$ dimensions, where one must also worry about the problem of simultaneously reproducing small and large distance structure in hadronic physics.

It may be useful to briefly consider the significant differences between the massive Schwinger model and all gauge theories in $3+1$ dimensions, to emphasize the intrinsic limitations on the lessons we can learn from this study. In $3+1$ dimensions ultraviolet (i.e., large transverse momenta) divergences appear, and the Hamiltonian must be allowed to "run" with the cutoffs. The gauge fields become dynamical, drastically increasing the size of the Fock space that must be considered to study even low-lying states. These dynamical gauge degrees of freedom have canonical couplings that lead to new infrared (i.e., small longitudinal momenta) divergences not seen in $1+1$ dimensions. The Tamm–Dancoff truncation violates rotational invariance. This immediately implies that the canonical Hamiltonian, which is constructed assuming that Lorentz covariance is maintained, must be supplemented with new "effective" interactions [30, 20, 31]. There are no calculations that indicate the Tamm–Dancoff limit, in which the cutoff on particle number is removed, can be taken; and only in the limit of small coupling constants can we support the hope that this limit will converge using Hamiltonians that closely resemble the canonical Hamiltonian. Added to these complications, in $3+1$ dimensions basis functions obviously depend on more variables, and we need more basis functions to span a richer space of low-lying states.

In the work presented here, we begin by truncating Fock space to two-particle ($f\bar{f}$) and four-particle ($f\bar{f}f\bar{f}$) sectors and by projecting the Einstein–Schrödinger equation onto these sectors to arrive at the coupled Tamm–Dancoff integral equations that govern them. We next choose a trial basis consisting of a finite number of functions that are not generally orthonormal. These are used to convert the integral equations into a simple matrix equation. The computer time required is dominated by the computation of matrix elements, each of which is a multi-dimensional integral. Therefore, the choice of an appropriate basis is driven by the need to reduce the time required to compute individual matrix elements and to reduce the number of

basis states (and thereby the number of matrix elements) required to obtain reasonable approximations. These are the numerical themes repeatedly emphasized in the text. Diagonalization of the resultant Hamiltonian matrix leads to our approximation for the spectra and wavefunctions of the low-lying states. The trial basis must be expanded until the numerical results converge. Richardson extrapolation [32] can be exploited to determine the rate of convergence and to improve results.

It is essential that we include the four-particle sector, because the first excited state of the theory is purely four-body in the massless limit and makes a smooth transition to being purely two-body in the limit of infinite mass. When $m_f = 0$, the ground state boson is a pure two-particle state and the first excited state corresponds to two free bosons with zero relative momentum. As the mass increases, the two bosons begin to interact, forming a state that can be efficiently described as a bound state of two bosons. As the mass increases further, a transition region occurs in which the predominantly four-particle state changes smoothly into a two-particle state that eventually bears no resemblance to a two-boson bound state. The eigenvalues of both states change smoothly, and as one expects from simple quantum mechanical arguments, there are no crossover effects in the transition region. The transition region is followed by the large fermion mass limit in which both the ground state and first excited state become increasingly two-body and increasingly non-relativistic. In this limit, the ground state mass approaches $2m_f$, the nonrelativistic limit. For all values of the fermion mass we find that the ground state contains a negligibly small four-particle component ($< 0.4\%$).

With an appropriate basis, our results accurately approximate the known exact results when $m_f = 0$; i.e., the theory is equivalent to a free theory of bosons with physical mass $M = e/\sqrt{\pi}$ [10]. The trial wave function methods leads to the exact results in this limit, as Bergknoff showed [15], because the exact wave functions are extremely simple in LFFT. Both DLCQ [22, 23] and lattice calculations [28] confront easily understood problems in this limit. As the fermion mass grows, the trial wave function chosen by Bergknoff in some of his calculations must be generalized; however, all the low-lying states become purely two-particle in nature and it is possible to use extremely simple trial wave functions to obtain accurate results for all values of the fermion mass. When the low-lying states are dominated by the two-body components, there are many other accurate numerical techniques one can choose [29]. Both DLCQ and the lattice become increasingly accurate as m_f increases.

Using Jacobi polynomials with a weight function chosen to provide the correct behavior for the amplitudes near the edges of momentum space or chosen to minimize the mass, we can readily reproduce, and often improve, all other numerical results for the low-lying states throughout the range of fermion mass. The ground state can be accurately reproduced using a single polynomial if the weight function is approximately adjusted, and the first excited state is accurately reproduced using approximately 20 or fewer polynomials. This result is encouraging, because the number of degrees of freedom and variables grows tremendously when one goes to QCD in $3 + 1$ dimensions, and we need to successfully reproduce hadrons using a small number of appropriately chosen basis functions.

This paper is organized into three sections. In Section 2 the coupled integral equations for the two- and four-particle amplitudes are derived from the light-front Einstein–Schrödinger equation. The numerical problem is to approximate the coupled integral equations (9) and (10) as matrix equations by finding appropriate basis functions. The primary constraints on the basis functions are that they allow fast computation of the multi-dimensional integrals that lead to matrix elements and that they be "close" to the exact eigenstates so that a small number of basis states can provide an accurate approximation. Most of the discussion of basis functions, and the presentation of results, is found in Section 3. We concentrate on the masses and eigenstates of the first two states for arbitrary fermion mass.

2. THE SCHWINGER MODEL LFTD EQUATIONS

The starting point for our bound state study in light-front field theory is the quantized version of Einstein's relation $P^2 = M^2$, the Einstein–Schrödinger equation in light-front coordinates,

$$M^2 |\psi\rangle = 2P^+ P^- |\psi\rangle. \tag{1}$$

Here, P^+ is the light-front momentum operator and P^- is the light-front Hamiltonian. We adopt the notational conventions of Ref. [8]. Unless otherwise specified, throughout the rest of this paper we will work with momentum eigenstates so that P^+ can be replaced by its eigenvalue, $\mathscr{P}$. Equation (1) is not a practical starting point for numerical calculations, because $|\psi\rangle$ is an infinite dimensional state vector. We make an approximation that must be justified a posteriori, letting $|\psi\rangle = |\psi_2\rangle + |\psi_4\rangle$, so that the wavefunction is truncated to allow only two- and four-particle components. Since the operator P^- has a lower bound for fixed $\mathscr{P}$, we will at least obtain an upper bound on the energy of the first two states of the theory using this approximation.

P^- is obtained using canonical quantization at equal light-front "time," $x^+ = \sqrt{1/2}\,(t + x)$. We work in light-cone gauge, so that $A^+ = \sqrt{1/2}\,(A^0 + A^1) = 0$ and $A^- = \sqrt{1/2}\,(A^0 - A^1)$ is a constrained variable that is eliminated using the classical equations of motion. Expanding the fermion field operators in a plane wave basis with $b^\dagger$ being

a fermion creation operator and $d^\dagger$ being an antifermion creation operator, the Hamiltonian is

$$P^- = P^-_{\text{free}} + P^-_{\text{self}} + P^-_0 + P^-_2, \tag{2}$$

where

$$P^-_{\text{free}} = \frac{m_f^2}{4\pi}\int_0^\infty \frac{dk}{k^2}\,[b^\dagger(k)\,b(k) + d^\dagger(k)\,d(k)], \tag{3}$$

$$P^-_{\text{self}} = \frac{e^2}{8\pi^2}\left\{\int_0^\infty \frac{dk_1}{k_1}\,[b^\dagger(k_1)\,b(k_1) + d^\dagger(k_1)\,d(k_1)] \times \int_0^\infty dk_2 \left[\frac{1}{(k_1-k_2)^2} - \frac{1}{(k_1+k_2)^2}\right]\right\}, \tag{4}$$

$$\begin{aligned} P^-_0 = \frac{e^2}{8\pi^3}\int_0^\infty \frac{dk_1\,dk_2\,dk_3\,dk_4}{\sqrt{k_1k_2k_3k_4}} &\times \Big\{[-b^\dagger(k_1)\,b^\dagger(k_3)\,b(k_2)\,b(k_4) \\ &- d^\dagger(k_2)\,d^\dagger(k_4)\,d(k_1)\,d(k_3)] \\ &\times \frac{\delta(k_1-k_2+k_3-k_4)}{2(k_1-k_2)^2} \\ &+ b^\dagger(k_1)\,d^\dagger(k_4)\,b(k_2)\,d(k_3)\,\frac{\delta(k_1-k_2-k_3+k_4)}{(k_1-k_2)^2} \\ &+ b^\dagger(k_1)\,d^\dagger(k_2)\,d(k_3)\,b(k_4)\,\frac{\delta(k_1+k_2-k_3-k_4)}{(k_1+k_2)^2}\Big\}, \end{aligned} \tag{5}$$

$$\begin{aligned} P^-_2 = \frac{e^2}{8\pi^3}\int_0^\infty \frac{dk_1\,dk_2\,dk_3\,dk_4}{\sqrt{k_1k_2k_3k_4}} &\times \Big\{[b^\dagger(k_1)\,b^\dagger(k_3)\,d^\dagger(k_4)\,b(k_2) \\ &- d^\dagger(k_2)\,d(k_1)\,d(k_3)\,b(k_4)] \\ &\times \frac{\delta(k_1-k_2+k_3+k_4)}{(k_1-k_2)^2} \\ &- [d^\dagger(k_2)\,b^\dagger(k_3)\,d^\dagger(k_4)\,d(k_1) \\ &- b^\dagger(k_1)\,b(k_2)\,d(k_3)\,b(k_4)] \\ &\times \frac{\delta(k_1-k_2-k_3-k_4)}{(k_1-k_2)^2}\Big\}. \end{aligned} \tag{6}$$

P^-_{free} is the free part of the Hamiltonian. P^-_{self} consists of self-induced inertias for the fermion and antifermion, which arise from normal-ordering. P^-_0 contains the interactions that do not change particle number. These include instantaneous photon exchange between fermions and/or antifermions, as well as an interaction in which a pair annihilates into an instantaneous photon at one vertex while another pair is created at the second vertex. P^-_2 contains the interactions in which the particle number is changed by two. These include interactions in which a fermion–antifermion pair annihilates into an instantaneous photon or vice versa at one vertex, with the instantaneous photon attaching to a fermion or antifermion at the other vertex. There are singularities in the Hamiltonian that ultimately cancel against one another, but some care is required to ensure that these cancellations are exact. This issue is discussed below.

The wavefunction $|\psi\rangle$ can be expanded,

$$\begin{aligned} |\psi\rangle = |\psi_2\rangle + |\psi_4\rangle = &\int_0^{\mathscr{P}} \frac{dk_1\,dk_2}{2\pi\sqrt{k_1k_2}} \\ &\times \delta(k_1+k_2-\mathscr{P})\,\psi_2(k_1,k_2)\,b^\dagger(k_1)\,d^\dagger(k_2)\,|0\rangle \\ &+ \frac{1}{2}\int_0^{\mathscr{P}} \frac{dk_1\,dk_2\,dk_3\,dk_4}{(2\pi)^2\sqrt{k_1k_2k_3k_4}}\,\delta\left(\sum_{i=1}^4 k_i - \mathscr{P}\right) \\ &\times \psi_4(k_1,k_2,k_3,k_4)\,b^\dagger(k_1)\,b^\dagger(k_2)\,d^\dagger(k_3)\,d^\dagger(k_4)\,|0\rangle, \end{aligned} \tag{7}$$

where ψ_2 and ψ_4 are the two- and four-particle amplitudes, respectively. Note that we can use Fermi statistics to choose ψ_4 to satisfy

$$\begin{aligned} \psi_4(k_1,k_2,k_3,k_4) &= -\psi_4(k_2,k_1,k_3,k_4) \\ &= -\psi_4(k_1,k_2,k_4,k_3) \\ &= \psi_4(k_2,k_1,k_4,k_3). \end{aligned} \tag{8}$$

Of course, the eigenstates automatically satisfy Fermi statistics, but the calculation is more efficient if we are able to choose a basis that manifestly satisfies Eq. (8).

It is convenient to scale the momentum $\mathscr{P}$ out of the problem by changing variables to momentum fractions, $x_i = k_i/\mathscr{P}$. When we project Eq. (1) onto free two- and four-particle states, we are led to the coupled equations,

$$\begin{aligned} \frac{M^2}{2}\psi_2(x,1-x) = &\frac{m_f^2}{2}\frac{1}{x(1-x)}\psi_2(x,1-x) \\ &+ \frac{e^2}{2\pi}\int_0^1 dy\,\psi_2(y,1-y) + \frac{e^2}{2\pi}\int_0^1 dy \\ &\times \frac{1}{(x-y)^2}\,[\psi_2(x,1-x) - \psi_2(y,1-y)] \\ &+ \frac{e^2}{\pi}\int_0^1 dy_1\,dy_2\,dy_3\,\delta_{y_1+y_2+y_3,x} \\ &\times \frac{\psi_4(y_1,y_2,y_3,1-x)}{(x-y_1)^2} \\ &- \frac{e^2}{\pi}\int_0^1 dy_2\,dy_3\,dy_4\,\delta_{y_2+y_3+y_4,1-x} \\ &\times \frac{\psi_4(x,y_2,y_3,y_4)}{[(1-x)-y_4]^2} \end{aligned} \tag{9}$$

and

$$\frac{M^2}{2}\psi_4(x_1, x_2, x_3, x_4)$$
$$= \frac{m_f^2}{2}\sum_{i=1}^{4}\frac{1}{x_i}\psi_4(x_1, x_2, x_3, x_4)$$
$$+\frac{e^2}{4\pi}\left\{\psi_2(x_2, 1-x_2)\left[\frac{1}{(x_1+x_3)^2}-\frac{1}{(x_1+x_4)^2}\right]\right.$$
$$+\psi_2(x_1, 1-x_1)\left[\frac{1}{(x_2+x_4)^2}-\frac{1}{(x_2+x_3)^2}\right]$$
$$+\psi_2(1-x_3, x_3)\left[\frac{1}{(x_1+x_4)^2}-\frac{1}{(x_2+x_4)^2}\right]$$
$$\left.+\psi_2(1-x_4, x_4)\left[\frac{1}{(x_2+x_3)^2}-\frac{1}{(x_1+x_3)^2}\right]\right\}$$
$$+\frac{e^2}{2\pi}\int_0^1 dy_1\, dy_2\left\{\delta_{y_1+y_2, x_1+x_2}\right.$$
$$\times\frac{\psi_4(y_1, y_2, x_3, x_4)-\psi_4(x_1, x_2, x_3, x_4)}{(x_1-y_1)^2}$$
$$+\delta_{y_1+y_2, x_3+x_4}\frac{\psi_4(x_1, x_2, y_1, y_2)-\psi_4(x_1, x_2, x_3, x_4)}{(x_3-y_1)^2}$$
$$+\delta_{y_1+y_2, x_1+x_4}\frac{\psi_4(y_1, x_2, y_2, x_3)-\psi_4(x_1, x_2, x_4, x_3)}{(x_1-y_1)^2}$$
$$-\delta_{y_1+y_2, x_2+x_4}\frac{\psi_4(y_1, x_1, y_2, x_3)-\psi_4(x_2, x_1, x_4, x_3)}{(x_2-y_1)^2}$$
$$-\delta_{y_1+y_2, x_1+x_3}\frac{\psi_4(y_1, x_2, y_2, x_4)-\psi_4(x_1, x_2, x_3, x_4)}{(x_1-y_1)^2}$$
$$+\delta_{y_1+y_2, x_2+x_3}\frac{\psi_4(y_1, x_1, y_2, x_4)-\psi_4(x_2, x_1, x_3, x_4)}{(x_2-y_1)^2}$$
$$-\delta_{y_1+y_2, x_1+x_4}\frac{\psi_4(y_1, x_2, y_2, x_3)}{(x_1+x_4)^2}$$
$$+\delta_{y_1+y_2, x_2+x_4}\frac{\psi_4(y_1, x_1, y_2, x_3)}{(x_2+x_4)^2}$$
$$+\delta_{y_1+y_2, x_1+x_3}\frac{\psi_4(y_1, x_2, y_2, x_4)}{(x_1+x_3)^2}$$
$$\left.-\delta_{y_1+y_2, x_2+x_3}\frac{\psi_4(y_1, x_1, y_2, x_4)}{(x_2+x_3)^2}\right\}, \qquad (10)$$

where $\delta_{x,y}\equiv\delta(x-y)$ and $\sum_{i=1}^4 x_i = 1$. Note that this last restriction implies that the space of free momentum fractions in the four-particle sector is three-dimensional; while the limitation $0<x_i<1$ for all i, implies that the allowed momentum fractions lie within a tetrahedron in this space. This constraint presents a severe problem if one tries to find a suitable orthonormal basis in the four-body space. We abandon orthonormality, complicating the ultimate matrix equation; however, this complication is easily justified because the solution of the final matrix equation represents a very small fraction of the total numerical effort.

Equations (9) and (10) have been written so that cancellations of divergences coming from the long-range Coulomb interaction in 1 + 1 dimensions are manifest. For example, in the third term on the right-hand side of Eq. (9) one can see that two linear divergences coming from P^-_{self} and P^-_0 cancel one another, leaving a finite result if one adopts a Cauchy principal value prescription for the remaining integral. This is what we do, and the principal values can be computed analytically in a basis function calculation.

By inspection, we can see that amplitudes $\psi_4(x_3, x_4, x_1, x_2)$ and $-\psi_2(1-x_1, x_1)$ satisfy Eqs. (9) and (10), if $\psi_4(x_1, x_2, x_3, x_4)$ and $\psi_2(x_1, 1-x_1)$ do. k_1 and k_2 are the coordinates of a particle and an antiparticle, respectively, in $\psi_2(k_1, k_2)$, and k_1 and k_2 are particle coordinates, while k_3 and k_4 are antiparticle coordinates in $\psi_4(k_1, k_2, k_3, k_4)$. Therefore, this observation is a consequence of charge conjugation symmetry, which remains valid after the Tamm–Dancoff truncation and implies that the wave functions can be chosen to be either symmetric or antisymmetric under charge conjugation. Thus, we are able to choose eigenstates that satisfy

$$\psi_2^{s,a}(1-x_1, x_1) = \mp\psi_2^{s,a}(x_1, 1-x_1),$$
$$\psi_4^{s,a}(x_3, x_4, x_1, x_2) = \pm\psi_4^{s,a}(x_1, x_2, x_3, x_4), \qquad (11)$$

where the upper signs correspond to symmetric (s) states and the lower signs to antisymmetric (a) states. Fermi statistics allow us to reduce the size of the Hamiltonian matrix by a factor of 16 (see Eq. (8)), and charge conjugation symmetry allows us to reduce its size by an additional factor of four.

3. SPECTRA AND WAVEFUNCTIONS

The LFTD integral equations, Eqs. (9) and (10), determine the spectra and wavefunctions of the truncated theory. In the massless limit, one can easily check that $\psi_2 = 1$ and $\psi_4 = 0$ is an eigenfunction of the coupled equations with eigenvalue $M = e/\sqrt{\pi}$. This is the ground state of the system with momentum $\mathscr{P}$, corresponding to a single boson of mass $e/\sqrt{\pi}$ and odd charge conjugation symmetry. With slightly more difficulty, it can be shown that $\psi_2 = 0$ and $\psi_4 = \sqrt{\delta(x_1-x_2-x_3+x_4)}-\sqrt{\delta(x_1-x_2+x_3-x_4)}$ is also an eigenstate of the theory with total momentum $\mathscr{P}$, even charge conjugation symmetry, and eigenvalue $M = 2e/\sqrt{\pi}$. Of course, the square root of a delta function must be inter-

preted using a suitable distribution. This is the first excited state of the system, corresponding to two free bosons each with mass $e/\sqrt{\pi}$ and with zero relative momentum. It is also straightforward to write the eigenstates with nonzero relative momentum. It is clear from the wave function that the bosons are free because there is no scattering term. We have chosen the norm of the two-boson state to be the same as the norm of the one-boson state, which is why we required a square root of a delta function in the four-particle amplitude. One can avoid such distributions by allowing states with different numbers of bosons to have different norms, but in our numerical calculations all states will have the same norm.

Before discussing the massive case, we should mention a few potentially confusing results from the massless calculation. Since we use a finite basis, we can produce only a discrete spectrum even when scattering states exist. Moreover, when one makes a Tamm–Dancoff truncation there are always spurious states that correspond to stable excitations of the fundamental boson and/or scattering states of such excitations. Consider what happens if we make the most severe truncation and allow only two-particle states. In this case, we exactly reproduce the boson of the theory, but we also find an infinite tower of excited two-particle states, which for brevity we will call "excitons." The first exciton has a mass approximately 2.43 times that of the ground state. Since there are no excited states of the fundamental boson according to the exact solution of the massless Schwinger model [10], this tower of discrete states is spurious. Bergknoff speculated [15] that these states disappear into the continuum when higher sectors of Fock space are retained, and a careful examination of the exact operator solution [15] reveals that this is indeed what happens. The excited two-particle states become components of the exact multi-boson states in the theory. The two-particle component of every multi-boson state is vanishingly small when the bosons are allowed to occupy plane wave states; however, a two-boson wave packet with unit norm, for example, typically has a non-vanishing two-particle component. Our basis states are incapable of producing a perfect plane wave, and the first excited state that we produce is always a wave packet of unit norm. Therefore, even in the limit where $m_f = 0$, our first excited state has a two-particle component that noticeably affects both the eigenvalue and the eigenstate.

When $m_f \neq 0$, we must compute the states numerically because the LFTD equations have not been solved analytically. The theory ceases to be equivalent to a theory of free massive bosons. In the bosonized theory, the bosons begin to interact [12, 13]. Since the interaction is attractive, one consequence of the interaction is that a two-boson bound state forms. Equivalently, the two-fermion and four-fermion sectors begin to mix and the first excited state of the theory has a mass that is less than twice the mass of the ground state. To see this we must solve Eqs. (9) and (10) simultaneously. To do this we choose an "appropriate" set of basis functions to expand the amplitudes ψ_2 and ψ_4. We take matrix elements of the Hamiltonian between all basis states, and since we do not assume that the basis states are orthonormal, we also take matrix elements of the identity. In this case, Eqs. (9) and (10) are replaced by a single matrix equation.

This scheme was recently used to find the low-lying two-fermion bound states in the $(1+1)$-dimensional Yukawa model, with a Tamm–Dancoff truncation that allows one virtual boson [21]. In the Yukawa model divergences occur, and numerical renormalization using sector-dependent counterterms was one of the primary concerns of this study. In the Yukawa model in this limited Fock space, as the fermion mass is reduced (i.e., strong coupling limit) the bound state mass actually becomes negative, so little effort was made to test the basis function method in the ultra-relativistic limit of the Yukawa model. In the massive Schwinger model we need not worry about divergences, once we have established all requisite cancellations, and sector-dependent counterterms exist in principle but are very small and can be ignored. Therefore we can concentrate on the new problems of including four-particle states efficiently and, more importantly, on the problem of producing accurate ultra-relativistic bound states in a theory in which this limit exists. In addition, there are numerical complications associated with instantaneous photon exchange that do not arise in the Yukawa model. These problems, discussed below, should play a major role in choosing a suitable basis for gauge theory calculations in $3+1$ dimensions also.

There are several factors that dictate the choice of basis functions. Physics determines what the exact eigenstates are, and one obvious criterion is that one wants to use as few simple basis functions as possible to accurately approximate the exact eigenstates. As the fermion mass changes, the eigenstates change drastically, and one must consider the possibility that different bases should be used for different masses. Since the number of matrix elements grows like the square of the number of basis functions, the need to keep this number small is obvious. However, for most basis functions that we studied the size of the matrix was not a limiting consideration. Most of the computer time was taken by the computation of the matrix elements themselves. The reason is simple. The matrix elements of P^- between two four-particle basis states involve four-dimensional integrals; e.g.,

$$\int_0^1 \prod_{m=1}^{4} dx_m\, dy_1\, dy_2\, \delta\left(\sum_{n=1}^{4} x_n - 1\right) \times \delta(x_1 + x_2 - y_1 - y_2)\, G_i(x_1, x_2, x_3, x_4) \times \frac{G_j(y_1, y_2, x_3, x_4) - G_j(x_1, x_2, x_3, x_4)}{(x_1 - y_1)^2}. \quad (12)$$

The basis functions will be discussed later, but it is the Coulomb interaction, $1/(x_1 - y_1)^2$, that prevents one from completing such integrals analytically for most basis functions. For most basis functions (e.g., Gaussians) it is necessary to perform this integration numerically. Our first calculations used numerical integration and included only one four-particle state, yet they required several hours of CPU time on a VAX 8650. We were forced to study *only basis functions for which all or most integrals can be computed analytically*. This is an extremely severe limitation. Beginning with a Laplace transform, it is possible to reduce the above integral to a one-dimensional integral if trigonometric or exponential functions are used. For Jacobi polynomials with a non-polynomial weight function all integrals can be computed analytically. In both cases the analytic expressions for the resultant matrix elements are tediously long and are most easily programmed by using deeply nested loops, which are not suitable if one needs to vectorize the calculation. Trigonometric and exponential basis functions suffer from more serious physical problems that we discuss below.

The only suitable basis functions that we discovered for ψ_2 and ψ_4 are products of Jacobi polynomials times a weight function, x^β. We use a product of polynomials and weight functions, one for each momentum fraction in the amplitude, and we fix β at a single value as discussed below. These functions were used by Bardeen, Pearson, and Rabinovici [33] in their transverse lattice studies of QCD_{3+1}. They are singled out because all integrals required to set up the matrix problem can be completed analytically, and we can choose β so that the amplitudes automatically vanish at the appropriate rate when any fermion momentum approaches zero. This is accomplished by letting $\beta = \sqrt{3/\pi}\,(m_f/e)$ for small fermion masses. The exact boundary condition is found by insisting that all singularities in Eqs. (9) and (10) coming from the regions of momentum space where $x_i \to 0$ cancel [27, 15]. This implies

$$\frac{\pi m_f^2}{e^2} - 1 + \pi\beta \cot(\pi\beta) = 0. \tag{13}$$

We should mention that the cancellation of these $x_i \to 0$ divergences is dynamical. If the fermion is massless, the light-front kinetic energy is zero and the Coulomb interaction leads to a substantial zero-momentum component in the wave function. When the fermion is massive, the kinetic energy goes like $1/x_i$, and it is the divergence of the kinetic energy that forces the wave function to vanish as $x_i \to 0$. It is interesting to note that DLCQ approximates all integrals using a multi-dimensional trapezoid rule with endpoints removed. This does not lead to any problems with respect to cancellations required to obtain the principal value for integrals like that in Eq. (12); however, it is difficult to obtain the correct end-point behavior of the wave-function when the fermion mass is small without using a large number of grid points [26, 21].

As the fermion mass becomes large we have found that the low-lying eigenvalues are much more easily reproduced if we use larger values of β than arise from Eq. (13), such as $\sqrt{3/\pi}\,(m_f/e)$. The low-lying states strongly peak where the total momentum can be equally shared between the constituents, and large values of β lead to basis functions that automatically satisfy this condition. If we choose β to minimize the mass with a single polynomial, we always improve the convergence of the calculations as the number of basis functions increases. In fact, as we will see below, it is only the four-particle sector that requires more than one polynomial if we wish to approximate the masses at the 1% level. If we do not choose β to minimize the energy, using Eq. (13), for example, increasingly large numbers of polynomials are required to reproduce even the ground state boson mass.

The main difficulties with using Jacobi polynomials plague most basis functions. It is possible to choose functions that are orthonormal in the two-particle sector, but since the three free momenta in the four-particle sector are constrained to lie inside a tetrahedron, it is quite tedious to construct an orthonormal basis in the four-particle sector. Instead we sacrifice orthonormality and solve a generalized Hamiltonian matrix equation, $H|\psi\rangle = EA|\psi\rangle$. Here A is an *overlap matrix* containing the matrix elements $\langle\phi_i|\phi_j\rangle$, where $|\phi_i\rangle$ is a basis state, and $|\psi\rangle$ is a vector composed of the coefficients of the basis states $|\phi_i\rangle$. When the determinant of A becomes small, roundoff errors can become significant. This turns out to be a secondary source of roundoff error and has not yet caused serious problems in our calculations. As we attempt to increase the number of Jacobi polynomial basis functions in the four-particle sector beyond ~ 30, we find that roundoff error becomes significant. This error results from the manner in which the analytic expressions for integrals in the matrix elements of the Hamiltonian, such as found in Eq. (12), are evaluated. For both polynomials and trigonometric functions it is most efficient to express the analytical solution in terms of a sum of terms, where the number of terms grows as the index on the basis function grows. In addition, for a polynomial basis, the magnitude of the individual terms in these sums grows as the index grows, and large cancellations occur. It may be possible to rewrite the analytic results to avoid such cancellations, but we have found no efficient way to do this. For the calculations presented here we never required more than 10 basis functions in the four-particle sector to obtain reasonable convergence for the first two eigenstates; and roundoff errors were not a serious problem.

Satisfying the boundary condition as any momentum vanishes, discussed above, is perhaps the most difficult constraint placed on a basis. This can be a serious problem for

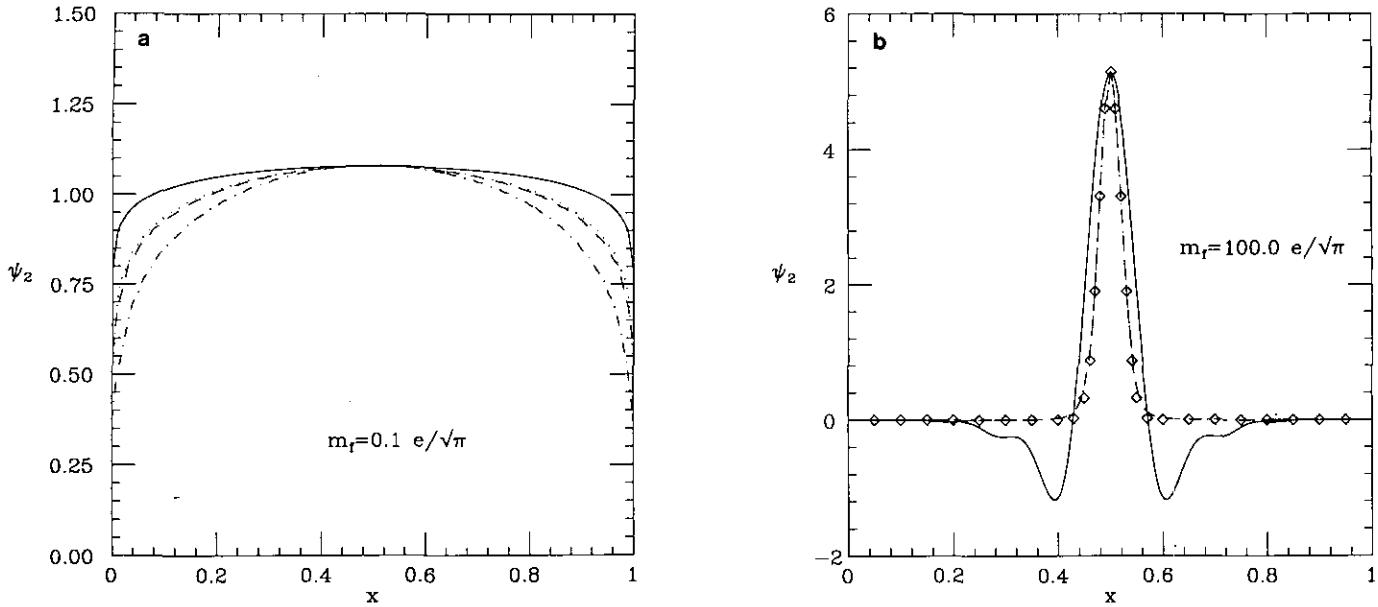

FIG. 1. *A comparison of the ground state two-particle component of the wave function, $\psi_2(x)$, from calculations using four different sets of basis functions.* (a) $m_f = 0.1e/\sqrt{\pi}$. The solid line is the result using 12 Jacobi polynomials with $\beta = \sqrt{3/\pi}\, m_f/e = 0.1\sqrt{3/\pi}$, the dotted using 60 trigonometric and exponential functions, the dashed using 60 cosines, and the dot-dashed using 60 sines. (b) Similar to (a) but for $m_f = 100.0e/\sqrt{\pi}$. Note that the dotted, dashed, and dot-dashed lines lie on top of one another. The solid line is the result of using 12 polynomials with $\beta = 8.0\sqrt{3/\pi}$, while the diamonds result from using a single polynomial with $\beta = 450.0\sqrt{3/\pi}$. The eigenvalues for both cases are shown in Table I.

light fermions even in the two-particle sector, where it is only necessary for the wave function to vanish at two points. Many trigonometric functions are required to produce a wave function that is nearly constant for all momenta except those near the edge of momentum space. As one can see in Fig. 1a, even 60 trigonometric basis functions cannot produce the eigenstate that is accurately reproduced by a few polynomials with the appropriate weight function. In Fig. 1a we show the result of using $\beta = \sqrt{3/\pi}\,(m_f/e)$ and 12 Jacobi polynomials; however, the wave function is reproduced quite well with a single polynomial [15]. In Fig. 2a we show how the eigenvalue changes with the number of basis functions in the two-particle sector for these same basis functions, and it is clear that the eigenvalue is reproduced with a single polynomial. Note that the results with trigonometric functions do not even appear to approach the correct limit. This is simply a result of the fact that it is not possible to produce a wave function that vanishes like x^β near $x = 0$ and like $(1-x)^\beta$ near $x = 1$ using any finite number of trigonometric and/or exponential functions. It is also an indication of how strongly these regions of momentum space are weighted in the exact mass. Using Richardson extrapolation we have numerically established that the error in a calculation with N trigonometric functions falls off like the inverse of Log(N). This is what one expects if the error is dominated by end-point behavior. It is possible to obtain an accurate extrapolation, but far more trigonometric functions than polynomials are required to obtain any specified accuracy.

A related, but different problem occurs for heavy fermions, as seen in Fig. 1b. Here the wave function approaches zero well away from the boundaries of momentum space because of the kinetic energy, P^-_{free} in Eq. (3). For the calculations with polynomials we encounter large roundoff errors when we use $\beta = \sqrt{3/\pi}\,(m_f/e)$ and are forced to use a smaller value such as $\beta = 8.0\sqrt{3/\pi}$. This error arises because of cancellations that occur in the analytic expressions we use for the Hamiltonian matrix elements. In this case many trigonometric functions produce a more accurate result than a few polynomials; however, when we use a program that can handle larger values of β, a single polynomial is capable of producing results as accurate as those obtained using large numbers of trigonometric functions, as shown by the single diamond in the lower left corner of Fig. 2b. This figure also shows that if β is not chosen appropriately, the polynomial basis calculations do not converge to the correct result as rapidly as the trigonometric basis calculations. Consideration of the wave function in Fig. 1b clarifies the problem. If β is not chosen sufficiently large, polynomials must be used to decrease the width of the wave function, and the required cancellations cannot be maintained by a few polynomials.

Such boundary problems are exacerbated in the four-particle sector where the wave function must vanish at the proper rate on all four faces of a tetrahedron. One cannot even produce a function that vanishes on these faces with a finite number of basis functions unless they vanish or approach a constant on these surfaces; of course, it is far

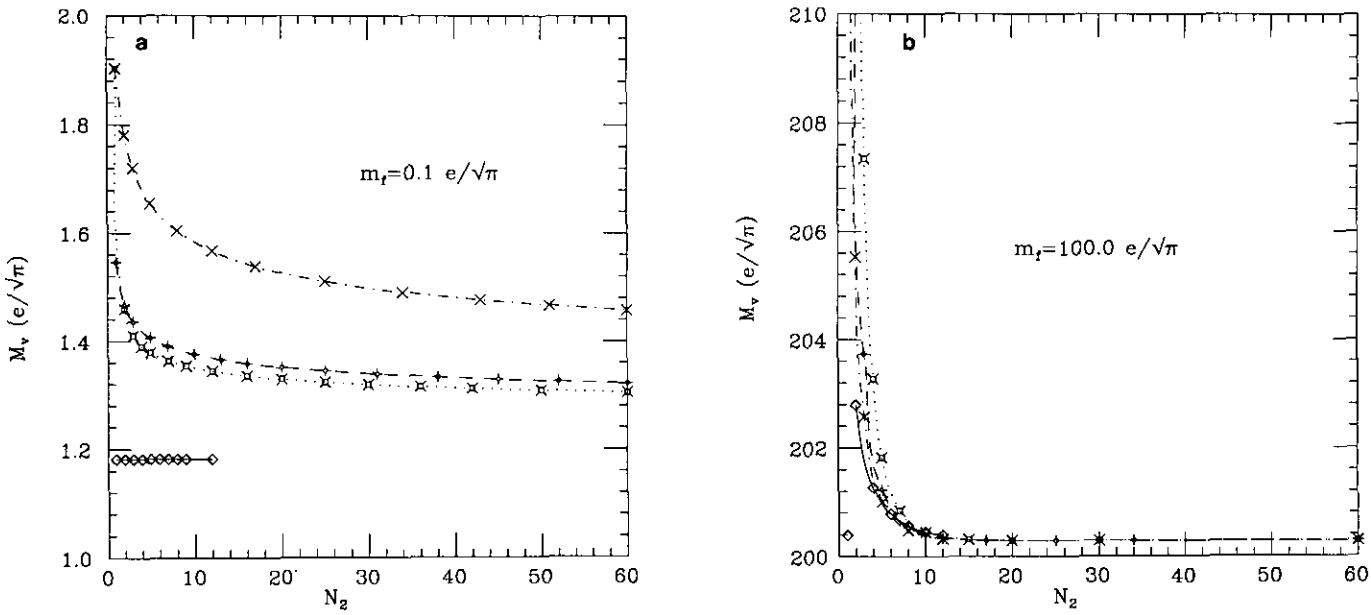

FIG. 2. Calculation of the ground state mass, M_v, as a function of the number of two-particle basis functions, N_2, using four different sets of basis functions. (a) $m_f = 0.1e/\sqrt{\pi}$. The short solid line is the result of using up to 12 Jacobi polynomials, the dotted using trigonometric and exponential functions, the dashed using cosines, and the dot-dashed using sines. (b) Similar to (a) but for $m_f = 100.0e/\sqrt{\pi}$. The solid line is again the result of using up to 12 polynomials with $\beta = 8.0\sqrt{3}/\pi$. The single point in the lower left corner is the result of using one polynomial with $\beta = 450.0\sqrt{3}/\pi$.

more difficult to produce functions that vanish at the appropriate rate. Trigonometric and exponential functions can be chosen to vanish on these surfaces; however, as should be clear from the simple two-particle examples shown in Figs. 1 and 2, it is not possible to use a small number of such functions and accurately approximate the power law behavior with which the exact eigenstates must vanish as the momentum of any constituent goes to zero. For small masses this problem becomes increasingly visible in the eigenvalues, and as discussed above these functions produce the correct limit only if the number of basis functions is allowed to become exponentially large.

To clarify this issue, consider the two-particle sector. A natural choice for the basis might be $\sin(k_n x_1)$, $\sin(k_m x_2)$, where x_1 and x_2 are the momentum fractions of the fermion and antifermion, respectively. These functions automatically vanish when either momentum goes to zero; however, they vanish far too rapidly when m_f is small. When $m_f = 0$ the lowest energy eigenstate is a constant, and an infinite number of sines are required to produce a constant. When m_f is small but nonzero, the amplitude must vanish at the endpoints, but no finite number of sines are able to accurately approximate the power law falloff implied by Eq. (13). If we expand our basis to include products of cosines, it is quite simple to obtain the exact ground state in the massless case, $\psi_2 = 1$; however, when $m_f \neq 0$ it is still impossible to produce the appropriate power law rise near $x = 0$ without using an exponentially large number of trigonometric basis functions.

In Table I we list numerical values for the ground state mass for five values of m_f. For $m_f = 0$ one obtains the exact result using either polynomials or cosines, but sines cannot accurately approximate this result. When the fermion mass is small but nonzero, only the polynomial bases produce acceptable results. As the fermion mass increases, all basis functions produce comparable results. Note that for all values of the fermion mass the ground state eigenvalue is given to better than 1% accuracy by a single polynomial when the weight function is chosen to minimize the mass.

Before discussing the results further, let us provide details concerning the basis function calculations in general and the polynomial basis functions in particular. Keeping in

TABLE I

Comparison of the Ground State Eigenvalues for Four Different Basis Functions

	Jacobi (1)	Jacobi (12)	Trig. & Exp. (60)	Cosine (60)	Sine (60)
$m_f = 0.0$	1.000	1.000	1.253	1.000	1.431
$= 0.1$	1.182	1.182	1.304	1.322	1.457
$= 1.0$	2.860	2.856	2.857	2.863	2.858
$= 10.0$	20.56	20.55	20.55	20.55	20.55
$= 100.0$	200.29	200.50	200.29	200.29	200.29

Note. In the first column, a single the function $x^\beta(1-x)^\beta$ is used with β adjusted to minimize the energy. In the second column, 12 Jacobi polynomials are used multiplying this weight function, with β adjusted as discussed in the text. The last three columns show the results of using various combinations of 60 trigonometric and exponential basis functions.

mind the symmetry requirements on $\psi_2(x, 1-x)$ and $\psi_4(x_1, x_2, x_3, x_4)$, we choose

$$\psi_2(x, 1-x) = \sum_k a_k \cdot F_k(x), \tag{14}$$

$$\psi_4(x_1, x_2, x_3, x_4) = \sum_{k_1, k_2, k_3} b_{k_1 k_2 k_3} \cdot G_{k_1 k_2 k_3}(x_1, x_2, x_3, x_4). \tag{15}$$

For the Jacobi polynomial basis

$$F_k(x) = [x(1-x)]^\beta P_k^{\beta,\beta}(2x-1) \tag{16}$$

and

$$\begin{aligned} &G_{k_1 k_2 k_3}(x_1, x_2, x_3, x_4) \\ &\quad = (x_1 x_2 x_3 x_4)^\beta P_{k_1}^{\beta,\beta}(x_1 + x_2 - x_3 - x_4) \\ &\qquad \times [P_{k_2}^{\beta,\beta}(x_1 - x_2 - x_3 + x_4) P_{k_3}^{\beta,\beta}(x_1 - x_2 + x_3 - x_4) \\ &\qquad - P_{k_3}^{\beta,\beta}(x_1 - x_2 - x_3 + x_4) P_{k_2}^{\beta,\beta}(x_1 - x_2 + x_3 - x_4)], \end{aligned} \tag{17}$$

where $P^{\beta,\beta}(x)$ is a Jacobi polynomial. We need to determine the coefficient vectors **a** and **b**. We have chosen $\beta = \sqrt{3/\pi}\,(m_f/e)$ in most examples, unless it is specified that β is chosen to minimize the energy. In general the values of β that minimize the energy are larger than $\sqrt{3/\pi}\,(m_f/e)$. The subscript k's on the Jacobi polynomials determine their order, and they must be chosen so that the symmetry relations (8) and (11) for $\psi_2^{s,a}(x_1, 1-x_1)$ and $\psi_4^{s,a}(x_1, x_2, x_3, x_4)$ are also satisfied by $F_k(x)$, $G_{k_1 k_2 k_3}(x_1, x_2, x_3, x_4)$.

With the expansions in Eqs. (14) and (15) for ψ_2 and ψ_4, we now multiply Eq. (9) by

$$\int_0^1 dx\, F_k(x),$$

and Eq. (10) by

$$\int_0^1 dx_1\, dx_2\, dx_3\, dx_4\, \delta\left(\sum_{j=1}^4 x_j - 1\right) G_{k_1 k_2 k_3}(x_1, x_2, x_3, x_4).$$

Using Eqs. (8) and (11) and simplifying, we obtain the matrix equation

$$\begin{aligned} &M^2 \begin{pmatrix} A^{(1)} & 0 \\ 0 & B^{(1)} \end{pmatrix} \begin{pmatrix} \mathbf{a} \\ \mathbf{b} \end{pmatrix} \\ &\quad = \begin{pmatrix} 2m_f^2 A^{(2)} + A^{(3)} - A^{(4)} & 4C^{(2)} \\ 4C^{(1)} & 4m_f^2 B^{(2)} + 2B^{(3)} + 4B^{(4)} - 4B^{(5)} \end{pmatrix} \\ &\qquad \times \begin{pmatrix} \mathbf{a} \\ \mathbf{b} \end{pmatrix}, \end{aligned} \tag{18}$$

where M is the mass of state and all masses are expressed in units of $e/\sqrt{\pi}$. The matrices $A^{(i)}$, $B^{(i)}$, and $C^{(i)}$ are

$$\begin{aligned} A_{ij}^{(1)} &= \int_0^1 dx\, F_i(x)\, F_j(x), \\ A_{ij}^{(2)} &= \int_0^1 dx\, \frac{1}{x} F_i(x)\, F_j(x), \end{aligned} \tag{19}$$

$$\begin{aligned} A_{ij}^{(3)} &= \int_0^1 dx\, dy\, F_i(x)\, F_j(y), \\ A_{ij}^{(4)} &= \int_0^1 dx\, dy\, F_i(x) \frac{F_j(y) - F_j(x)}{(x-y)^2}, \end{aligned} \tag{20}$$

$$C_{ij}^{(1)} = \int_{(4)} \frac{1}{(x_2 + x_4)^2} G_i(x_1, x_2, x_3, x_4)\, F_j(x_1) = C_{ji}^{(2)}, \tag{21}$$

$$B_{ij}^{(1)} = \int_{(4)} G_i(x_1, x_2, x_3, x_4)\, G_j(x_1, x_2, x_3, x_4), \tag{22}$$

$$B_{ij}^{(2)} = \int_{(4)} \frac{1}{x_1} G_i(x_1, x_2, x_3, x_4)\, G_j(x_1, x_2, x_3, x_4), \tag{23}$$

$$\begin{aligned} B_{ij}^{(3)} = \int_{(6)} &G_i(x_1, x_2, x_3, x_4) \\ &\times \frac{G_j(y_1, y_2, x_3, x_4) - G_j(x_1, x_2, x_3, x_4)}{(x_1 - y_1)^2}, \end{aligned} \tag{24}$$

$$\begin{aligned} B_{ij}^{(4)} = \int_{(6)} &\frac{1}{(x_1 + x_2)^2} \\ &\times G_i(x_1, x_4, x_3, x_2)\, G_j(y_1, x_4, x_3, y_2), \end{aligned} \tag{25}$$

$$\begin{aligned} B_{ij}^{(5)} = \int_{(6)} &G_i(x_1, x_4, x_3, x_2) \\ &\times \frac{G_j(y_1, x_4, x_3, y_2) - G_j(x_1, x_4, x_3, x_2)}{(x_1 - y_1)^2}, \end{aligned} \tag{26}$$

where

$$\begin{aligned} \int_{(4)} &\equiv \int_0^1 dx_1\, dx_2\, dx_3\, dx_4\, \delta\left(\sum_{k=1}^4 x_k - 1\right), \\ \int_{(6)} &\equiv \int_0^1 dx_1\, dx_2\, dx_3\, dx_4\, dy_1\, dy_2\, \delta\left(\sum_{k=1}^4 x_k - 1\right) \\ &\quad \times \delta(x_1 + x_2 - y_1 - y_2). \end{aligned}$$

We can now calculate these integrals and solve the matrix equation to obtain the spectrum and wavefunctions. The singularities in the multi-dimensional integrals found in Eqs. (20), (24), and (26) are regularized by imposing a

principal value prescription, after re-writing the integrals using

$$\int_0^1 dy \frac{F_j(y)-F_j(x)}{(x-y)^2} = \frac{1}{x(1-x)} F_j(x) - \int_0^1 dy \frac{1}{(x-y)} \frac{\partial F_j(y)}{\partial y} \quad (27)$$

and

$$\int_0^1 dy_1\, dy_2\, \delta(x_1+x_2-y_1-y_2) \times \frac{G_j(y_1, y_2, x_3, x_4) - G_j(x_1, x_2, x_3, x_4)}{(x_1-y_1)^2} = \left(\frac{1}{x_1}+\frac{1}{x_2}\right) G_j(x_1, x_2, x_3, x_4) - \int_0^1 dy_1\, dy_2 \frac{\delta(x_1+x_2-y_1-y_2)}{(x_1-y_1)} \times \left[\frac{\partial G_j(y_1, y_2, x_3, x_4)}{\partial y_1} - \frac{\partial G_j(y_1, y_2, x_3, x_4)}{\partial y_2}\right]. \quad (28)$$

After some tedious algebra, we obtain analytic solutions for all integrals in terms of gamma functions [33] and no singularities remain in the numerical calculation.

For $\psi_2(x)$ to satisfy Eq. (11), we must choose $k = 0, 2, 4, \ldots$ for the ground state, and $k = 1, 3, 5, \ldots$ for the first excited state, in the polynomials $P_k^{\beta,\beta}(x)$ that occur in the expansion of $\psi_2(x)$. As shown in Figs. 3a and b, the eigenvalue M converges very rapidly for both of these states as the number of basis functions in the two-particle sector increases for all three typical regions of fermion mass. In the following, we set $N = 8$ for the number of polynomials in the two-particle sector, because there is no noticeable improvement when $N > 8$.

Turning to the four-particle basis, Eqs. (8) and (11) require us to choose $k_1 = 0, 2, 4, \ldots$ and $k_2, k_3 = 1, 3, 5, \ldots$, or $k_1 = 1, 3, 5, \ldots$, and $k_2, k_3 = 0, 2, 4, \ldots$ for the ground state $G_{k_1 k_2 k_3}(x_1, x_2, x_3, x_4)$ (see Eq. (11)); and for the first excited state, we must have $k_1, k_2, k_3 = 0, 2, 4, \ldots$, or $k_1, k_2, k_3 = 1, 3, 5, \ldots$. Since the contribution of the four-particle amplitudes to the ground state is negligibly small (about 0.4% compared to that of the two-particle state), we will not discuss its small effect on the ground state. Its contribution to the first excited state can be seen from Figs. 4a and b, where the convergence of M as the number of the four-particle basis functions increases is shown. While it is not clear that M has converged in Fig. 4a, from Fig. 4b we can see that M does converge rapidly when we include the two-particle component of the eigenstate. This convergence is least rapid for the lightest fermion mass, which is also the state with the largest four-particle component. Convergence in the four-particle sector is never as rapid as in the two-particle sector because of the necessity to reproduce both the internal wave function of each of two bosons and to reproduce the wave function for the relative motion of these bosons. As we discuss in detail below, the latter wave function is strongly peaked in momentum space while the former is very broad for light fermions.

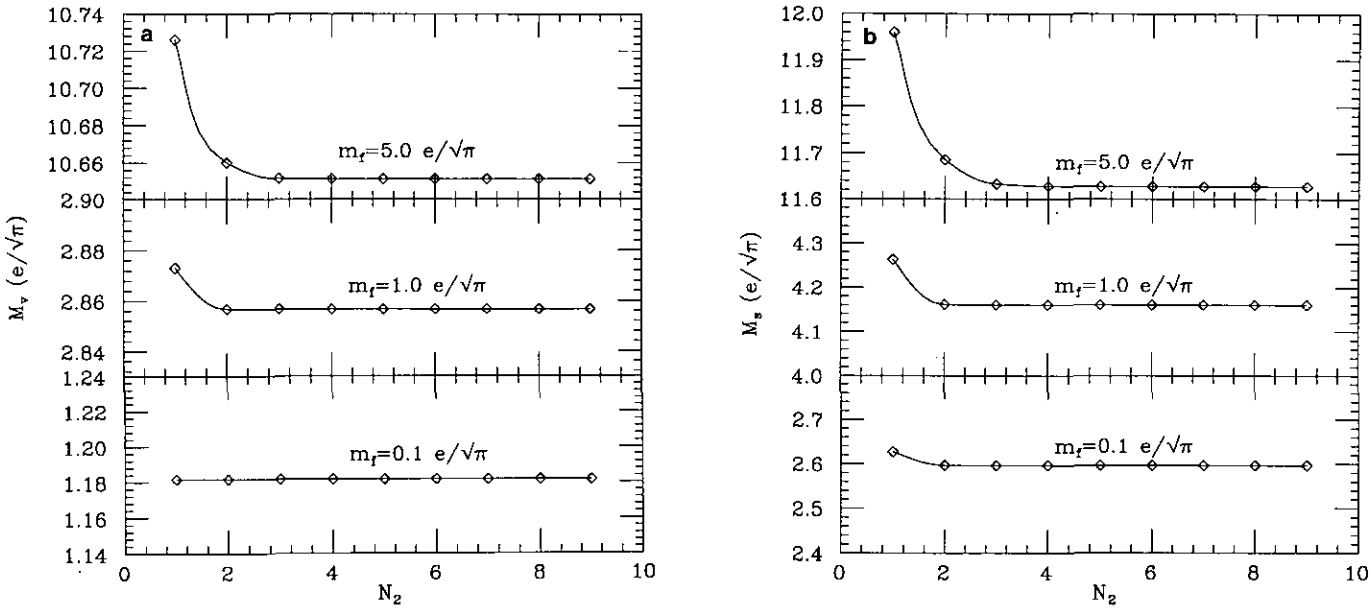

FIG. 3. (a) The ground state mass, M_v, as a function of the number of two-particle Jacobi polynomial basis functions, N_2, for three typical values of m_f. (b) Same as (a) except for the first excited state mass, M_s. No four-particle states are included in this calculation.

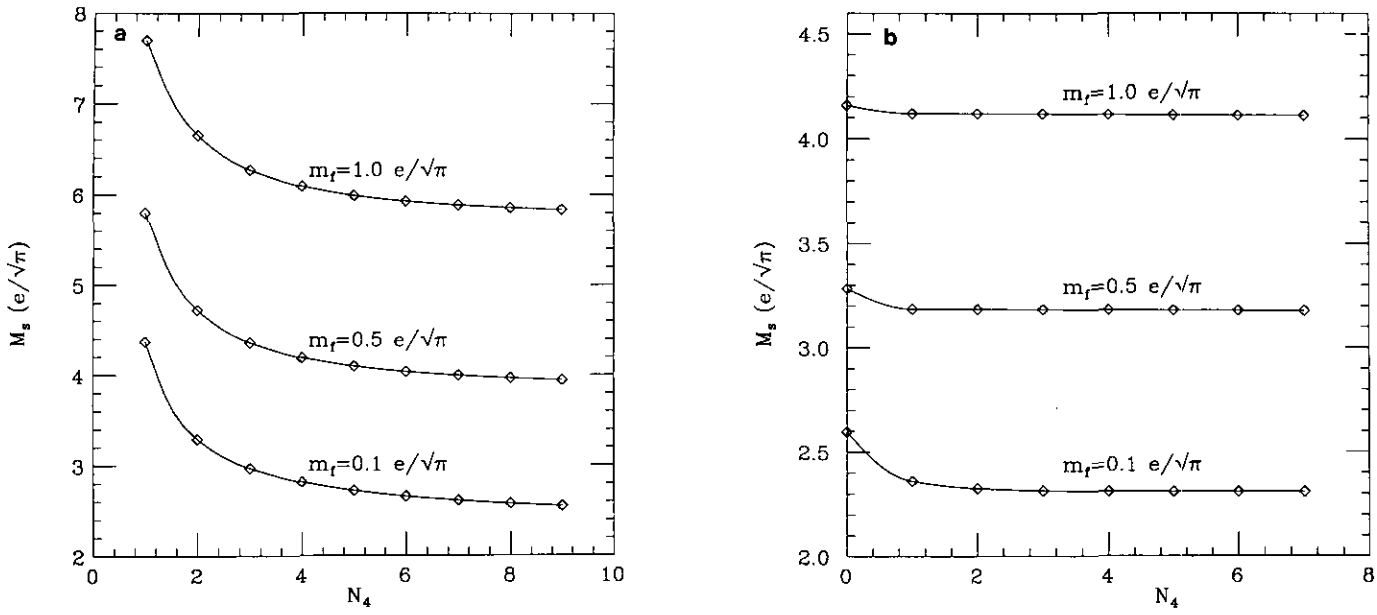

FIG. 4. (a) The first excited state mass, M_s, as a function of the number of four-particle Jacobi polynomial basis functions, N_4, for three typical values of m_f. No two-particle states are included in this calculation. (b) Same as (a) but with 8 two-particle states included.

Given $F_k(x)$ and $G_{k_1k_2k_3}(x_1, x_2, x_3, x_4)$, the relative contribution of the two- and four-particle states to the first excited state can be calculated, and the result is shown in Fig. 5. One clearly sees that as the fermion mass increases, the weakly bound two-boson state that is dominantly a four-particle state makes a steady transition to becoming a two-particle excited state that resembles a new stable boson. As $m_f \to 0$ one sees that in our calculations the first excited state does not become a pure four-particle excitation, always including at least a 30% two-particle contribution. As discussed above, it is not possible to produce a state in which bosons exactly share momentum (i.e., are at rest with respect to one another) in the small bases that we consider, and in the wave packets that can be formed there is a significant two-particle component even though the states are extremely close in mass to the scattering threshold. If one

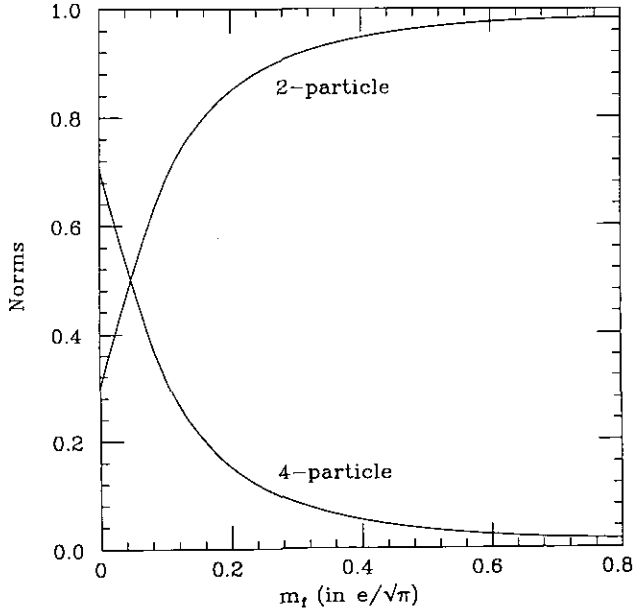

FIG. 5. The relative contribution of the two- and four-particle components to the first excited state as a function of m_f.

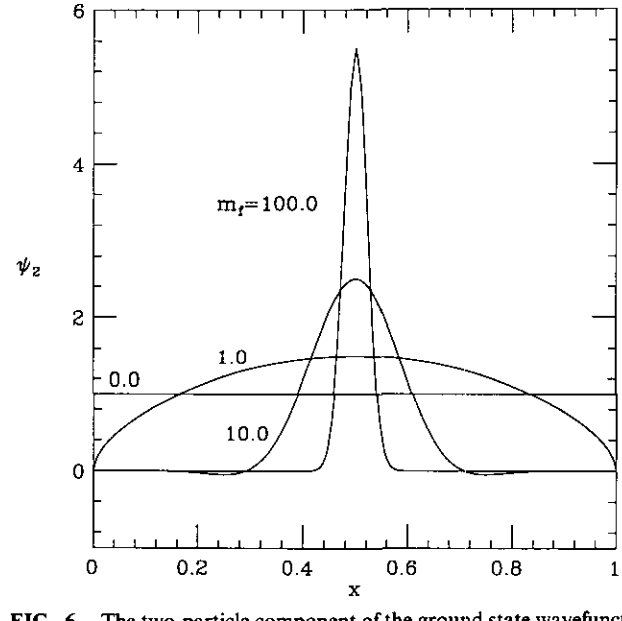

FIG. 6. The two-particle component of the ground state wavefunction for four typical values of m_f, which are given in units of $e/\sqrt{\pi}$. The norm is arbitrary.

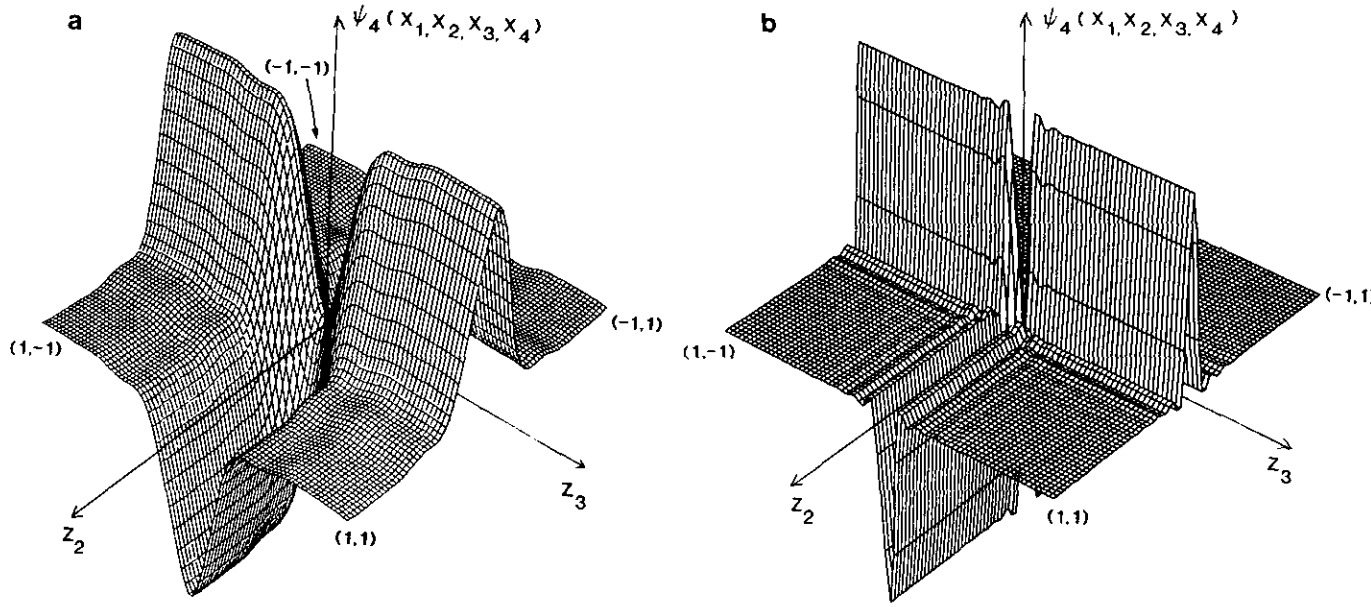

FIG. 7. The first excited state wavefunction, ψ_4, in the $m_f = 0.0$ limit. In this limit ψ_4 is a function of only two variables, $z_2 = x_1 - x_2 - x_3 + x_4$ and $z_3 = x_1 - x_2 + x_3 - x_4$. (a) Ten four-particle Jacobi polynomial basis functions are used to construct ψ_4, and 8 two-particle polynomials are included in the full state. The resultant mass is $M_s = 2.007e/\sqrt{\pi}$. (b) Same as (a) with 66 trigonometric basis functions in the four-particle sector and an additional 20 in the two-particle sector. The resultant mass is $M_s = 2.0005e/\sqrt{\pi}$.

forms a wave-packet using the exact operator solution [15], there is a significant two-particle contribution, so this "error" is entirely due to the problem of constructing a scattering state with a small basis.

In Fig. 6, we present the ground state wave function, $\psi_2(x)$. In these calculations we have dropped $\psi_4(x_1, x_2, x_3, x_4)$, because its presence produces no noticeable change in $\psi_2(x)$. The figure clearly shows the well-known behavior of the wave function for various masses. As $m_f \to 0$ the wave function becomes flat in momentum space. When the mass is small the wave function vanishes at the boundaries of momentum space as dictated by Eq. (13). As the mass increases the ground state wave function becomes increasingly peaked about $x = \frac{1}{2}$. All of these results agree with previous work [22, 28, 29].

For the first excited state, in the strong coupling or light fermion mass domain, the four-particle component of the wave function dominates and resembles two bound fermion–antifermion pairs. Each pair behaves as a relatively free massive boson [12, 13], with the boson–boson interaction vanishing as $m_f \to 0$. The mass of a two-boson state is minimized when their relative momentum vanishes, so that the two-boson wave function becomes a delta-function peaked around $x = \frac{1}{2}$, where x is the momentum fraction of a boson. While our small basis cannot produce a delta function, Fig. 7a clearly shows that the four-particle wave function is strongly peaked about $x_1 - x_2 + x_3 - x_4 = 0$ and $x_1 - x_2 - x_3 + x_4 = 0$. These two variables correspond to the two ways one can form fermion–antifermion pairs from the four particles, and one clearly sees that $\psi_4(x_1, x_2, x_3, x_4)$ is symmetric under charge conjugation, as required by Eq. (11) since the state is symmetric. Figure 8 shows the two-particle component when one retains the four-particle sector, along with the first excited two-particle state that

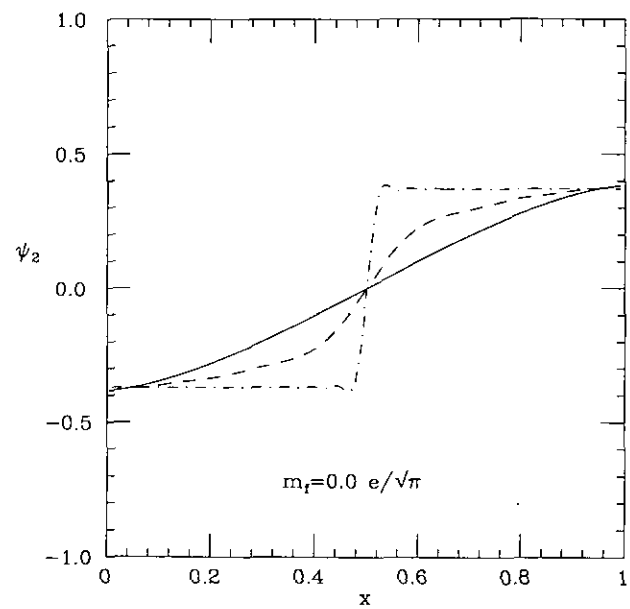

FIG. 8. The two-particle components for the first excited state in the $m_f = 0.0$ limit. The solid line results from dropping the four-particle component. The dashed line is the result with the four-particle component shown in Fig. 7a, while the dot-dashed line is the result with the four-particle component shown in Fig. 7b.

one obtains when the four-particle sector is removed. One sees that the first excited state of the two-particle system, as well as higher states, mix with the four-particle state to form the complete two-boson state. In units of $e/\sqrt{\pi}$ the excited state mass is $M = 2.007$, which should be compared to the exact result of $M = 2$. This result is excellent given the small number of basis functions used. The fermion and anti-fermion in each boson want to remain very close in position space, while the two bosons want to spread as broadly as possible in position space. The wave functions must simultaneously reproduce this disparate behavior.

Figure 7b shows the same projection of $\psi_4(x_1, x_2, x_3, x_4)$ shown in Fig. 7a but from a calculation using trigonometric functions. Using 66 cosines one is clearly better able to approximate the delta function required to minimize the kinetic energy coming from the relative motion of the two bosons. It is interesting to note that the norm of the two-particle component of the wave-function produced with Jacobi polynomials is 0.30, while this norm in the calculation using trigonometric functions is much closer to the exact value of 0, being 0.05. The mass is also more accurate, being $M = 2.0005$. This improvement is primarily due to the fact that many more basis functions are used, and it is deceptive because it only occurs when $m_f = 0$. In this single case the wave function is not required to vanish at the edges of momentum space and the cosines are not required to approximate the appropriate power law falloff of the wave functions. When m_f is small but non-zero, the mass estimate for the cosine basis is about 20% too large, a significant error. As mentioned above, there is a discontinuous jump in the mass estimate for the first excited state using this basis. It increases by roughly 20% when m_f is given any non-zero value.

When $m_f = 0$ the four-particle wave function depends only on the variables displayed in Figs. 7a and b; however, when $m_f \neq 0$, it depends on four variables. In this case we have chosen not to display the wave function; instead, we show how the physical masses behave over a large range of fermion masses. Figure 9 shows the mass of the ground state boson, M_v, and the first excited state, M_s, as a function of the fermion mass m_f. The ground state curve (dash-dot line) is obtained from the calculation of pure two-particle or mixed two- and four-particle amplitudes. The difference would not be noticeable in this figure, illustrating the negligible effect of the four-particle sector for the ground state over a broad range of fermion masses. The dotted line shows the first excited state mass when the state is restricted to the four-particle sector, while the dashed line shows this mass when the state is restricted to the two-particle sector. The solid line shows the mass when both sectors are retained. For large fermion masses one clearly sees that the mass is approximated quite well by the two-particle calculation, because the full excited state is almost purely two-particle. At $m_f = 0$, where the excited state should be purely four-particle one sees that the four-particle calculation does produce a lower mass than the two-particle calculation; however, as discussed above, our basis functions are not

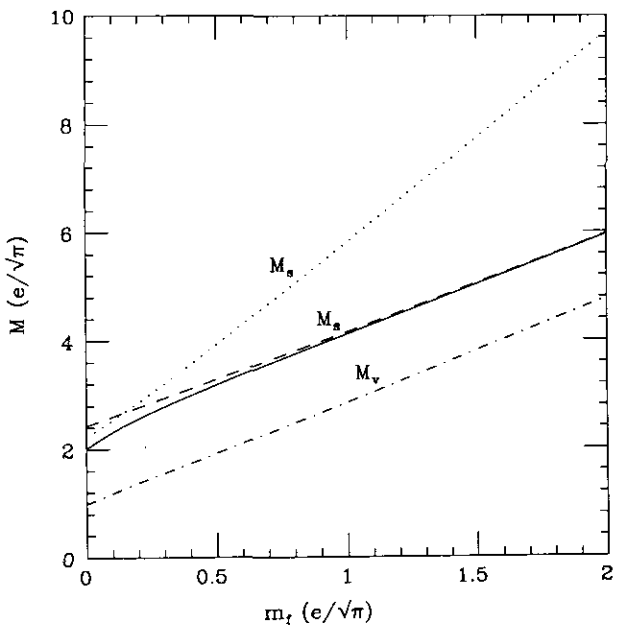

FIG. 9. The masses of the ground state, M_v, and first excited state, M_s, as a function of m_f. The dot-dashed line shows M_v, which is not noticeably affected by the four-particle component. The dotted line shows M_s from a calculation with four-particle and no two-particle components, while the dashed line shows M_s from a calculation with two-particle and no four-particle components. The solid line indicates the results when both two-particle and four-particle components are retained in the first excited state.

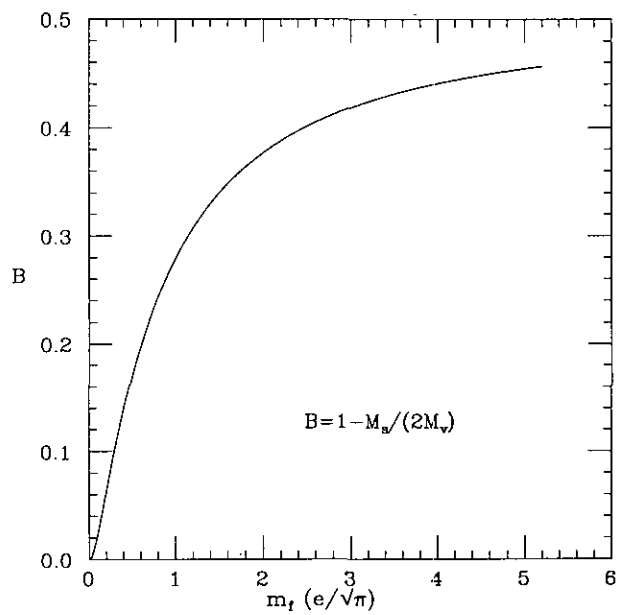

FIG. 10. The binding energy of the first excited state as a function of m_f.

able to produce a four-particle state corresponding to two bosons perfectly at rest with respect to one another, and the dotted line does not precisely meet the solid line because of this problem. For all small masses energy minimization guarantees that the solid line will lie below both the dashed and dotted line. The mass clearly changes smoothly through the transition region in which the excited state is changing from a four-particle to a two-particle state.

With M_v and M_s available, we can calculate the binding energy B of the first excited state, defined by $B = 1 - M_s/(2M_v)$. This is shown in Fig. 10. In the $m_f \to 0$ limit, the binding energy goes to zero while in the $m_f \to \infty$ limit, B approaches $\frac{1}{2}$. In the region between, the transition is smooth, and we can compute it accurately through the entire range of masses using a single set of basis functions. The behavior shown in this figure is exactly what one expects in the bosonized theory, where the two bosons forming the bound state are attracting one another with an increasingly strong force, and in the fermion theory, where the two-particle excited state moves downward in mass from the continuum as the individual fermion masses increase. Of course the wave functions provide far more information, allowing one to compute any observable of interest, such as charge form factors.

In Table II we provide a comparison with previous numerical results [22, 28]. We show all results in the units chosen in Ref. [21], i.e., in units of $\sqrt{m_f^2 + e^2/\pi}$. There is no variational principle for the lattice calculations, so a comparison of these results with ours does not immediately indicate which is more accurate. There is an approximate minimization principle for DLCQ, and one sees that our results agree with the DLCQ results for most values of m_f. The discrepancy increases at the smallest values of the fermion mass, and here we believe our results because they smoothly approach the analytic results at $m_f = 0$. Note that for the lightest fermion masses our ground state results agree quite well with the lattice results, while our results for the excited state differ noticeably from these. We believe that errors arise in the lattice calculations because of the necessity to simultaneously produce small and large distance behavior in the excited state. This problem does not arise for the ground state because here the fermion–antifermion pair effectively sit on top of one another in the massless limit (in light-front coordinates), so that it is only necessary to accurately reproduce short distance behavior.

In summary, the LFTD equations for the massive Schwinger model can be readily solved for the low-lying eigenvalues and eigenstates using polynomial basis functions in the two-particle and four-particle sectors of Fock space. It is possible to produce accurate, convergent eigenvalues and eigenstates for all values of the fermion mass, from weak through strong coupling, using relatively few (~ 10) basis functions in each sector. In the more interesting case of QCD in $3+1$ dimensions, we must deal with a higher number of dimensions, dynamical gluons, extra internal variables (e.g., color, flavor, and spin), and an entirely new set of renormalization problems. It is essential that we be able to approximate hadron wave functions using relatively few basis states for the spatial part of the wave functions, and our results for the massive Schwinger model are encouraging.

TABLE II

Comparison of Basis Function Results for the Ground State and the First Excited State Masses, $M_{v,s}$, with Equal-Time Lattice Calculations [28], M_{+-}, and with DLCQ Calculations [22], $M_{1,2}$

m_f/e	M_-	M_1	M_v	M_+	M_2	M_s
2^5	2.006	2.006	2.006	2.014	2.014	2.014
2^4	2.014	2.013	2.014	2.036	2.033	2.034
2^3	2.032	2.030	2.031	2.109	2.081	2.082
2^2	2.067	2.064	2.064	2.212	2.188	2.188
2^1	2.122	2.114	2.114	2.453	2.399	2.401
2^0	2.143	2.129	2.129	2.777	2.723	2.717
2^{-1}	1.990	1.975	1.974	2.852	2.956	2.920
2^{-2}	1.653	1.675	1.653	2.625	2.936	2.803
2^{-3}	1.367	1.476	1.368	2.353	2.868	2.542

Note. All results are given in units of $\sqrt{m_f^2 + e^2/\pi}$.

ACKNOWLEDGMENTS

We thank Avaroth Harindranath and Junko Shigemitsu, who initiated the study of the Schwinger model using basis functions and provided invaluable assistance throughout the course of this work. We also thank Kent Hornbostel and Wei-Min Zhang for helpful discussions. This work was supported in part by the National Science Foundation under Grant PHY-9102922 and the Presidential Young Investigator Program through Grant PHY-8858250 (RJP), and by a grant from Cray Research, Inc.

REFERENCES

1. An extensive list of references on light-front physics (*light.tex*) is available via anonymous ftp from public.mps.ohio-state.edu in the subdirectory tmp/infolight. Among these, Refs. [15, 8] below may serve as introductions for this paper.
2. P. A. M. Dirac, *Rev. Mod. Phys.* **21**, 392 (1949).
3. I. Tamm, *J. Phys. (USSR)* **9**, 449 (1945).
4. S. M. Dancoff, *Phys. Rev.* **78**, 382 (1950).
5. G. Feldman, T. Fulton, and J. Townsend, *Phys. Rev. D* **7**, 1814 (1973).
6. A. Harindranath and J. P. Vary, *Phys. Rev. D* **37**, 1064 (1988).
7. R. J. Perry, A. Harindranath, and K. G. Wilson, *Phys. Rev. Lett.* **65**, 2950 (1990).
8. R. J. Perry and A. Harindranath, *Phys. Rev. D* **43**, 4051 (1991).
9. J. Schwinger, *Phys. Rev.* **125**, 397 (1962); **128**, 2425 (1962).
10. J. Lowenstein and A. Swieca, *Ann. Phys. (N.Y.)* **68**, 172 (1971).
11. G. McCartor, *Z. Phys. C* **52**, 611 (1991).

12. S. Coleman, R. Jackiw, and L. Susskind, *Ann. Phys. (N.Y.)* **93**, 267 (1975).
13. S. Coleman, *Ann. Phys. (N.Y.)* **101**, 239 (1976).
14. See, for example, K. G. Wilson and J. Kogut, *Phys. Rep. C* **12**, 75 (1974).
15. H. Bergknoff, *Nucl. Phys. B* **122**, 215 (1977).
16. A. Harindranath and J. P. Vary, *Phys. Rev. D* **37**, 3010 (1988).
17. St. Glazek, *Phys. Rev. D* **38**, 3277 (1988).
18. C. Dietmaier, T. Heinzl, M. Schaden, and E. Werner, *Z. Phys. A* **334**, 215 (1989).
19. K. Hornbostel, *Phys. Rev. D* **45**, 3781 (1992).
20. R. J. Perry and K. G. Wilson, "Perturbative Renormalizability with an Infinite Number of Relevant and Marginal Operators," Ohio State preprint, 1993 (unpublished).
21. A. Harindranath, R. J. Perry, and J. Shigemitsu, *Phys. Rev. D* **46**, 4580 (1992).
22. T. Eller, H.-C. Pauli, and S. J. Brodsky, *Phys. Rev. D* **35**, 1493 (1987).
23. T. Eller and H. C. Pauli, *Z. Phys. C* **42**, 59 (1989).
24. C. M. Yung and C. J. Hamer, *Phys. Rev. D* **44**, 2598 (1991).
25. For a fairly complete list of DLCQ references see Ref. [1] above, or S. J. Brodsky and H. C. Pauli, "Light-Cone Quantization and Quantum Chromodynamics," Invited Lecture at the 30th Schladming Winter School, SLAC-PUB-5558, 1991.
26. J. R. Hiller, *Phys. Rev. D* **44**, 2504 (1991).
27. G. t'Hooft, *Nucl. Phys. B* **75**, 461 (1974).
28. D. P. Crewther and C. J. Hamer, *Nucl. Phys. B* **170**, 353 (1980).
29. Y. Ma and J. R. Hiller, *J. Comput. Phys.* **82**, 229 (1989).
30. For a simple example, see S. D. Glazek and R. J. Perry, *Phys. Rev. D* **45**, 3740 (1992).
31. R. J. Perry, "A Renormalization Group Approach to Hamiltonian Light-Front Field Theory," Ohio State preprint, 1993 (unpublished).
32. See, for example, G. Dahlquist and A. Björck, *Numerical Methods* (Prentice–Hall, London, 1969).
33. W. A. Bardeen, R. B. Pearson, and E. Rabinovici, *Phys. Rev. D* **21**, 1037 (1980).